*Short Communication*

# Electrodeposition of Gold Nanoparticles on Electrochemically Reduced Graphene Oxide for Sensitive Hydrazine Electrochemical Determination in Agriculture Wastewater

*Xiaohui Lu[1,*], Peifang Wang[1], Xianguo Wang[3] and Yongbin Guo[4]*

[1] School of Earth science and engineering,Ministry of Education Key Laboratory of Integrated Regulation and Resource Development on Shallow Lakes, Hohai University, Nanjing, Jiangshu, 210098, China.
[2] Ministry of Education Key Laboratory of Integrated Regulation and Resource Development on Shallow Lakes, Hohai University, Nanjing, Jiangshu, 210098, China
[3] Henan Provincial Bureau of Geology and mineral resources, Jinshui Road 28, Zhengzhou, 450012, China
[4] Nanjing Hydraulic Research Institute, 223 Guangzhou Road, Nanjing, 210029, China.
[*]E-mail: luxiaohui945@hhu.edu.cn

In this contribution, reduced graphene oxide-gold nanoparticles nanocomposite (RGO-AuNPs) was prepared by electrochemical reduction of graphene oxide (GO) at an indium tin oxide (ITO) electrode followed by an electrodeposition process of loading AuNPs on its surface. The electrochemical reduction and deposition progress were characterized by various techniques including SEM, XRD, UV-vis spectroscopy and Raman spectroscopy. As-prepared RGO-AuNPs modified ITO was then successfully applied for electrochemical determination of hydrazine. Results indicate that the RGO is a perfect platform for AuNPs deposition. The composite material exhibits a superior electrocatalytic property towards detection of hydrazine. Moreover, the proposed sensor was successfully used for real water sample analysis.

**Keywords:** Graphene; Gold nanoparticle; Electrochemical; Electrodeposition; Hydrazine

## 1. INTRODUCTION

Hydrazine is a common reagent used in the chemical industry. It has wide application in many products such as emulsifier, reducing agent, corrosion inhibitor, stabilizer and catalyst. It also is a starting component for several insecticide, herbicide and pesticide production. Moreover, hydrazine also used in some formula for pharmaceutical drug usage [1]. Due to the excellent anti-poisoning

ability in fuel electro-oxidization process, hydrazine also known as a good candidate in direct fuel cell system [2]. However, hydrazine is a toxic chemical reagent not only could harmful human health also threat environment. Therefore, developing a reliable technique for sensitive determination of hydrazine is essential [3]. Many techniques have been already studied for detecting hydrazine. These methods include flow injection analysis [4], ion chromatography [5], chemiluminescence (CL) and spectroscopy based methods [6, 7]. Although these methods could be applied for hydrazine detection in some degree, the extremely complex preparation procedure, long time analysis period, narrow detection range and expensive instrument still problems for making them towards real application. In order to overcome these problems, electrochemical method was proposed for hydrazine analysis due to its portable, quick and low cost. On the other hand, electrochemical method also suffers from its own disadvantage due to the kinetically sluggish of hydrazine. High detection overpotential is required using commercial carbon based electrode. In order to overcome this disadvantage, researchers proposed several approaches in an attempt to reduce the overpotential and enhance the electro-oxidation signal. Studies found the most effective approach is the electrode surface modification using specifically chosen redox material. Besides, several metal based electrode also could directly apply for electrochemical hydrazine analysis such as platinum [8], rhodium [9] and palladium [10] due to their excellent electrocatalytic properties.

Graphene is a 2D $sp^2$-hybridised carbon lattice with a single atom thickness. Graphene is common platform material for noble metal nanoparticle deposition and form superior composite material due to its unique structure [11-14]. Using graphene as a platform is better than other material due to its excellent properties such as high specific surface area, high electron mobility, electrical conductivity and mechanical property [15]. Graphene oxide (GO) is a oxidize state of graphene, which synthesized using graphite under strong oxidation conditions. GO is the number one choice for a solution based method for preparing graphene based composite. GO could firstly couple with target material and then reduced by reducing agent [16, 17]. For example, Feng and co-workers [18] demonstrated a poly(vinylpyrrolidone)-assisted method for synthesizing Au@Pd nanoflowers deposited on reduced GO (RGO). As prepared Au@Pd/RGO was used for fuel-cell applications. More specifically, GO, $Pd^{2+}$ and $Au^{3+}$ were reduced together using formic acid as reducing agent under a hydrothermal condition. Au@Pd/RGO nanocomposite was also prepared by a one-pot approach using trisodium citrate and ascorbic acid as additives [19]. The synthesized Au@Pd/RGO nanocomposite was then applied for electrochemical application. Lu and co-workers also prepared an Au@Pd/RGO nanocomposite using PVP as a capping agent [20, 21]. Their Au@Pd/RGO nanocomposite exhibited a superior oxygen-reduction reaction activity. A similar Au@Pd/RGO nanocomposite was successfully prepared by Xu et al. [22]. In this case, GO was used as a surfactant for controlling growth of Au@Pd. $NaBH_4$ was acting as a reducing agent and the entire reaction was conducted in an oil bath for 24 h at 100 °C. They then explored the superior photocatalytic property of Au@Pd/RGO nanocomposite.

In this paper, we reported the electrodeposition of AuNPs on the electrochemically RGO using GO and $HAuCl_4$ as precursors. The entire fabrication process was conducted on a glassy carbon electrode modification. The prepared RGO-AuNPs nanocomposite was then used as a good candidate for hydrazine detection. Results indicate the RGO-AuNPs nanocomposite modified GCE have an excellent electrocatalytic property towards detection of hydrazine. It also exhibits excellent stability

and anti-interference property. Moreover, the proposed sensor was successfully used for real water sample analysis.


## 2. EXPERIMENTAL

Modified Hummers method was used for GO preparation by strong oxidize graphite [23]. In a typical process, 4 g graphite powder was put into 60 mL of concentrated $H_2SO_4$ and then add 1.25 g $NaNO_3$. After gentle mixing, 15 g of $KMnO_4$ was then added followed by mixing. In order to increase the reaction temperature, the entire process was conducted in an ice bath. Then, the mixture was stirred at 40 °C for 1 h. After that, 200 mL water was added and the temperature of the solution was increased to almost boiling. This condition was kept for half hour. Then, the reaction was terminated by adding 500 mL of water with certain of $H_2O_2$ solution. Centrifugation was used for separating solid sample from the solution. Wash and re-disperse process was repeated until all impurities were removed. The solid sample was then dried in a vacuum oven. $HAuCl_4$ were were purchased from Sigma-Aldrich.

In our electro-reduction process of GO, ITO was chosen as the conductive substrate for fabricating GO film. Specifically, 5 mL GO solution (1 mg/mL) was drop coated on an ITO and dried in an oven. The GO reduction process was conducted using CV scanning from 0 to −1.3 V in $N_2$ saturated PBS solution for 150 scan cycles. RGO/ITO was rinsed with water to remove the PBS. Result RGO dispersion was collected by sonication of RGO/ITO in a bath sonicator for 30 min.

For glassy carbon electrode modification, 5 μL of RGO dispersion (1 mg/mL) was dropped onto the GCE surface and dried at room temperature. The electrochemical deposition of AuNPs was performed in 1 M $H_2SO_4$ solution containing 1% $HAuCl_4$ using chronoamperometry at an applied potential of −0.2 V for 120s. A CH Instruments 660A electrochemical Workstation was used for all electrochemical experiments. Three electrode system was used for the experiment. An Ag/AgCl (3M KCl) as the reference electrode and a platinum electrode was used as the auxiliary electrode. For real sample test, the agriculture wastewater samples were collected from a local nursery (Greenwood Inc.) in Nanjing. For anti-interference test, $PdCl_2$, $ZnNO_3$ and CuO was used as $Pd^{2+}$, $Zn^{2+}$ and $Cu^{2+}$ sources and dissolved in water to prepare 1 mM solution, respectively. Glucose and ascorbic acid was directly dissolved in water to prepare 1 mM solution. For stability, RGO-AuNPs/GCE was prepared for detecting 0.1 mM hydrazine every 3 days over a month. After each detection, the RGO-AuNPs/GCE was stored in a 2 °C refrigerator.

A Hitachi S-4800 (Hitachi, Japan) scanning electron microscope (SEM) was used for observing structure and morphology of prepared RGO and RGO-AuNPs nanocomposite. The Raman spectra of GO and RGO-AuNPs nanocomposite was analyzed using a Raman microscope (Renishaw, inVia) with 514 nm laser light at room temperature. The surface functional group status of the GO and RGO-AuNPs was collected using a Fourier transform infrared spectroscopy (FTIR, Nicolet iS5, Thermo Scientific). XPS in a VG Multilab2000 spectrometer was used for analysing the formation of metallic Au. Uv-vis spectra of the GO, RGO and RGO-AuNPs nanocomposite was collected by a UV-vis spectrophotometer (Perkin Elmer Lambda 950).
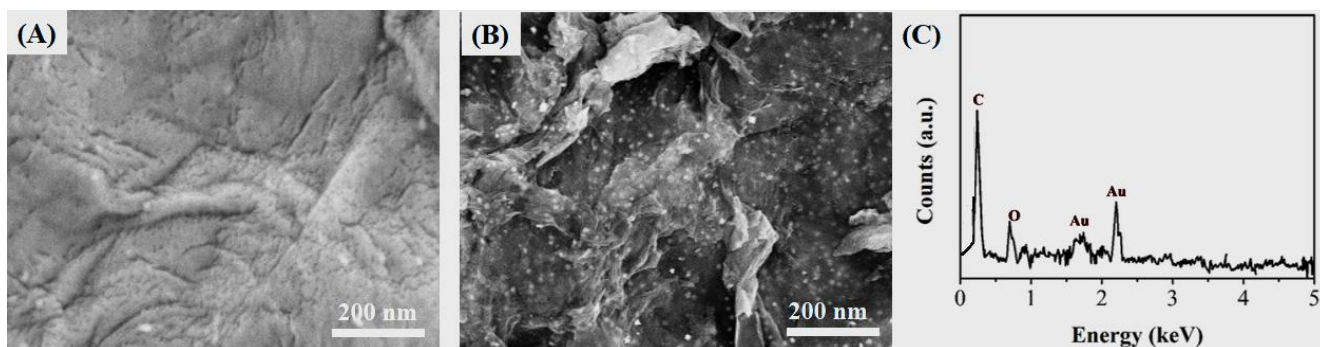
## 3. RESULTS AND DISCUSSION



**Figure 1.** SEM images of (A) RGO and (B) RGO-AuNPs nanocomposite. (C) EDX spectrum of RGO-AuNPs nanocomposite.

Surface morphology of the RGO and RGO-AuNPs nanocomposite was observed using SEM. Figure 1A and B show the typical SEM observation of electrochemically reduced GO and RGO-AuNPs nanocomposite under the same magnification. As shown in the figure, the RGO displays a flake-like structure with many wrinkles. The surface of the sample is very smooth without any break, which is commonly observed in chemically reduced GO. After chronoamperometric deposition of AuNPs (Figure 1B), uniform decoration of AuNPs can be observed on the surface and interlayer of RGO. Based on 200 individual AuNPs measurements, the average size of the AuNPs is 39 nm. We also collected the SEM image using high EHT voltage level to visualize the uniformity of the AuNPs, which suggested the chronoamperometric deposition method could uniformly deposit AuNPs on the electrochemically reduced GO film without aggregation.
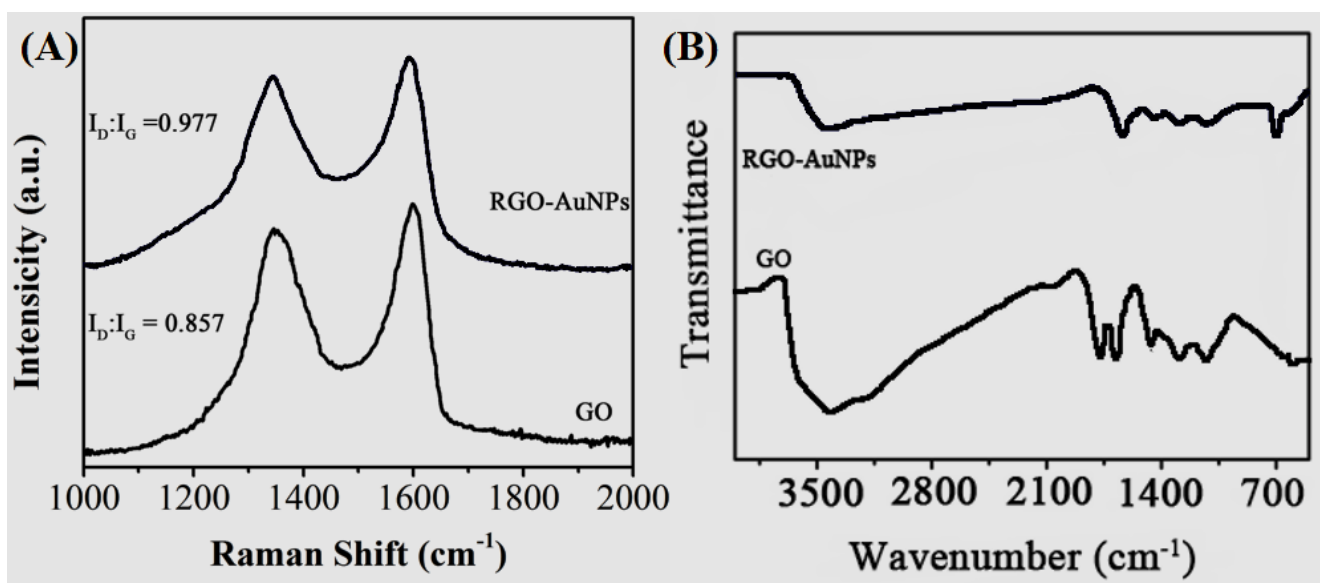


**Figure 2.** (A) Raman and (B) FTIR spectra of GO and RGO-AuNPs nanocomposite.

The elemental information of prepared RGO-AuNPs nanocomposite was confirmed by EDX. Figure 1C shows the EDX spectrum of RGO-AuNPs nanocomposite and indicates the presence of elemental C, O and Au signals. The signals of C and Au can be originated from RGO and AuNPs, respectively. The signal of O can be ascribed from two aspects, the absorbed $O_2$ and the existence of oxygen containing surface functional groups of RGO which have not been fully reduced using CV scans. It can be observed no other impurity element in the RGO-AuNPs nanocomposite, suggesting the formed nanocomposite had high purity. Therefore, using our proposed method for preparing RGO-AuNPs nanocomposite is a reliable method.

The electrochemical reduction of GO needs to be confirmed by characterizations. The crystal structure change of GO during the reduction process was confirmed by Raman spectroscopy analysis. Figure 2A shows the Raman spectra of GO and RGO-AuNPs nanocomposite. As can be observed, both spectra exhibit two characteristic bands at 1345 and 1592 cm$^{-1}$, which can be assigned to the D and G bands, respectively. D band is due to the first-order scattering of $E_{2g}$ phonons by sp$^2$ carbon atoms while G band is due to the breathing mode of κ-point photons of $A_{1g}$ symmetry [24]. The intensity change of the ratio of the D and G band can be used for analyzing the surface status change of the GO. In our case the intensity ratio of the D and G peaks increases from 0.857 to 0.977 for the RGO-AuNPs nanocomposite, indicating the restoration of sp$^2$ domains on reduction under CV scan condition.

FTIR characterization was also used for GO reduction process confirmation. As shown in the Figure 2B, the FTIR of GO shows peaks at 3419, 1724, 1402, 1222 and 1062 cm$^{-1}$, which reflect the OH stretching, C=O stretching, OH deformation, epoxy C–O stretching vibration and alkoxy C–O stretching vibration, respectively [25]. After electrochemical reduction process, the peak at 1724 cm$^{-1}$ shows disappearing. The oxygen containing functional groups also show a significant decreasing. Moreover, after reduction, no signal of the epoxy C–O stretching vibration of GO can be observed, indicating the successful removal of the oxygenated groups. In addition, a strong C=C stretching peak at 1635 cm$^{-1}$ coupled with appearance of doublet peaks at 2935 and 2860 cm$^{-1}$ (symmetric and antisymmetric stretching vibrations of –CH$_2$ group, respectively) could be observed after electrochemical reduction, suggesting the restoration of the carbon basal plane in RGO [26].
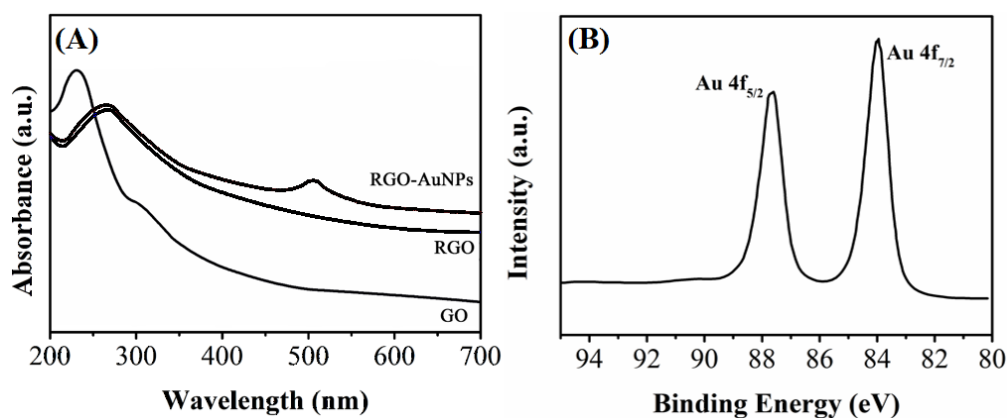


**Figure 3.** (A) UV-vis spectra of GO, RGO and RGO-AuNPs nanocomposite (B) Au 4f narrow XPS scan of the RGO-AuNPs nanocomposite.

The reduction process was also confirmed by the UV-vis spectroscopy analysis. As shown in Figure 3A, the UV-vis spectrum of GO dispersion shows a clear absorption peak at 288 nm with large shoulder peak around 317 nm. These two peaks could assign to the aromatic C—C bonds from $\pi$—$\pi^*$ transitions and C=O bonds from n—$\pi^*$ transitions, respectively [27]. On the other hand, the RGO displays a different spectrum, the absorption peak red shifts to 275 nm. Moreover, the spectrum shows a clear increasing in visible range, indicating the GO was the electronic conjugation within the RGO sheets was restored upon electrochemical reduction, further confirm the GO reduced during the electrochemical reduction process [28]. From the analysis of RGO-AuNPs nanocomposite, the formation of AuNPs also can be confirmed. As shown in the spectrum, after deposition of AuNPs, the spectrum of the nanocomposite shows a new broad absorption peak centred at about 510 nm, corresponding to the surface plasmon absorption of Au nanoparticles, confirming the existence of Au nanoparticles in the sample [29].

The formation of AuNPs then confirmed by XPS analysis. Figure 3B shows an Au 4f XPS spectrum of RGO-AuNPs nanocomposite. The Au $4f_{7/2}$ peak appeared at a binding energy of 84.11 eV and the Au $4f_{5/2}$ peak appeared at a binding energy of 87.91 eV. This indicates the formation of metallic gold [30, 31].
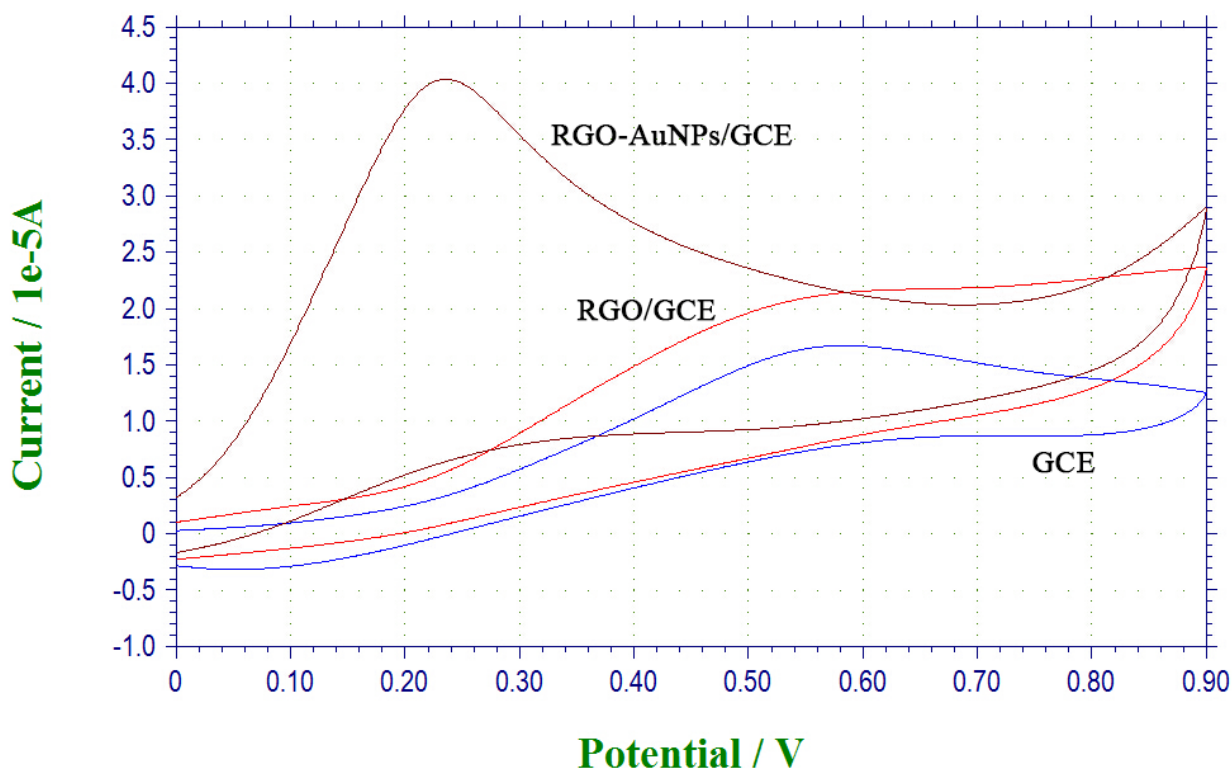


**Figure 4.** CV scans of 0.1 mM hydrazine using GCE, RGO/GCE and RGO-AuNPs/GCE.

The electrocatalytic performance of the RGO-AuNPs nanocomposite towards hydrazine electro-oxidation in PBS was studied by cyclic voltammetry. Figure 4 shows the CV scans of 0.1 mM hydrazine in PBs using GCE, RGO/GCE and RGO-AuNPs/GCE. It can be seen that the higher oxidation peak current was obtained using RGO-AuNPs/GCE with low overpotential for hydrazine. In

contrast, bare GCE shows a very small oxidation peak at X V for hydrazine electro-oxidation. RGO/GCE shows a small enhancement but remains a similar overpoential. Therefore, it can be concluded that the electro-oxidation process of hydrazine can be electro-catalyzed by RGO-AuNPs/GCE.

The scan rate effect of electrochemical determination performance was studied. We scanned the RGO-AuNPs/GCE in PBS in the presence of 0.1 mM hydrazine at different scan rates. Results indicate that the electro-oxidation current response was linearly proportional to the square root of the scan rate, which indicated the hydrazine reaction at the electrode surface is controlled by the diffusion process.

The pH effect of electrochemical determination performance was studied as well. We studied the CV scans of using RGO-AuNPs/GCE in PBS in presence of 0.1 mM hydrazine at different pH condition. The results suggest the current response of the hydrazine increases from pH 2 to 5 and then decreases after further increasing pH. Therefore, pH 5 was selected for optimum condition.

The detection range and detection limit of the RGO-AuNPs/GCE towards hydrazine was obtained by DPV method. As shown in the Figure 5, the RGO-AuNPs/GCE had a linear detection performance towards hydrazine from 0.1 μM to 0.2 mM. The detection limit can be calculated as 0.02 μM based on signal to noise of 3. We then compared our results to several recent literatures and summarized in Table 1. As shown in the comparison results, the analytical performance of RGO-AuNPs/GCE towards hydrazine is comparable with other results, indicating our proposed method can be potentially used for real application.
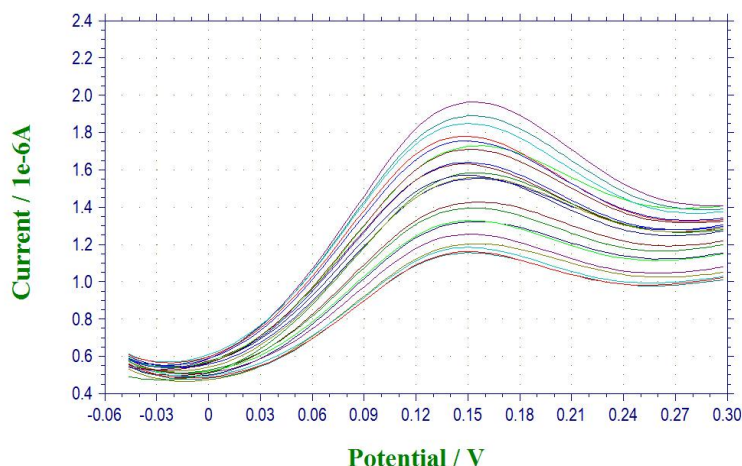


**Figure 5.** DPV of RGO-AuNPs/GCE for the successive addition of hydrazine.

**Table 1.** Comparison of hydrazine electrochemical sensors.

| Electrode | LDR[a] (μM) | LOD[b] (μM) | Reference |
|---|---|---|---|
| ZnO nanonails | 0.1-1.2 | 0.02 | [32] |
| ZnO nanoflowers | 0.6-250 | 0.18 | [33] |
| PSS-graphene | 3-300 | 1.00 | [34] |
| NiTsPc-titanized silica | 0.1-0.6 | 0.01 | [35] |
| RGO-AuNPs/GCE | 0.1-200 | 0.02 | This work |

We tested the reliability of proposed hydrazine electrochemical sensor. The RGO-AuNPs/GCE was used for determination of hydrazine in real agriculture waste water sample by PDV measurement. The standard addition method was adopted for examining the recovery of hydrazine in water samples. The results of real sample determination was summarized in Table 2.

**Table 2.** Determination of hydrazine in agriculture wastewater samples using RGO-AuNPs/GCE.

| Sample | Added (nM) | Found (nM) | Recovery (%) | RSD (%) |
|--------|-----------|-----------|-------------|---------|
| Sample 1 | 0 | 0 | — | 0.01 |
| Sample 2 | 20 | 17.07 | 95.4 | 1.51 |
| Sample 3 | 50 | 50.30 | 102.7 | 0.09 |
| Sample 4 | 100 | 101.20 | 102.1 | 1.01 |

Possible interferences for the determination of hydrazine at the RGO-AuNPs/GCE was tested by the addition of different compound species such as $Cu^{2+}$, $Zn^{2+}$, $Pd^{2+}$ into pH 5.00 PBS in the presence of 0.1 mM hydrazine. As shown in Table 3, the results indicated that these compound species did not show clear interference.

**Table 3.** Anti-interferences test using RGO-AuNPs/GCE.

| Interference species | Current change (%) |
|---------------------|-------------------|
| $Cu^{2+}$ | 1.20 |
| $Zn^{2+}$ | 2.07 |
| $Pd^{2+}$ | 0.87 |
| Glucose | 1.22 |
| Ascorbic acid | 2.47 |

The stability of RGO-AuNPs/GCE was tested every 3 days in a month. The current response to 0.1 mM hydrazine declined about 17% after a month (Table 4), indicating the proposed sensor had qualified stability.

**Table 4.** Stability test of RGO-AuNPs/GCE for detecting 0.1 mM hydrazine over a month.

| Day | Current response (%) | Day | Current response (%) |
|-----|---------------------|-----|---------------------|
| 3 | 100 | 6 | 94.7 |
| 9 | 93.6 | 12 | 91.0 |
| 15 | 91.0 | 18 | 90.7 |
| 21 | 88.5 | 24 | 86.9 |
| 27 | 85.3 | 30 | 83.2 |

## 4. CONCLUSION

In summary, RGO-AuNPs nanocomposite was prepared by electrochemical reduction of GO at an ITO electrode followed by an electrodeposition process of loading AuNPs on its surface. The

synthesized RGO-AuNPs nanocomposite was characterized by SEM, Raman spectroscopy, UV-vis spectroscopy and XPS, and then employed successfully applied for electrochemical determination of hydrazine in agriculture wastewater.

**Reference**

1. B. Zhou, J. YangandX. Jiang, *Mater. Lett.*, 159 (2015) 362
2. W. Ding, M. Wu, M. Liang, H. NiandY. Li, *Analytical Letters*, 48 (2015) 1551
3. Z. Zhao, Y. Sun, P. Li, S. Sang, W. Zhang, J. HuandK. Lian, *Journal of The Electrochemical Society*, 161 (2014) B157
4. R.B. Channon, M.B. Joseph, E. Bitziou, A.W. Bristow, A.D. RayandJ.V. Macpherson, *Anal. Chem.*, 87 (2015) 10064
5. E. Gionfriddo, A. Naccarato, G. SindonaandA. Tagarelli, *Anal. Chim. Acta.*, 835 (2014) 37
6. Y. Su, Y. Xie, X. HouandY. Lv, *Applied Spectroscopy Reviews*, 49 (2014) 201
7. S. Pattanayak, A. Swarnkar, A. PriyamandG.M. Bhalerao, *Dalton Transactions*, 43 (2014) 11826
8. C.-h. Chen, L. Jacobse, K. McKelvey, S.C. Lai, M.T. KoperandP.R. Unwin, *Anal. Chem.*, (2015)
9. J.-M. Yan, H.-L. Wang, Z.-L. WangandQ. Jiang, *Journal of power sources*, 262 (2014) 386
10. S. Ye, H. Wang, Q. Xiao, Q. DingandJ. Wu, *Advanced Synthesis & Catalysis*, 356 (2014) 3225
11. S. Dutta, C. Ray, S. Sarkar, M. Pradhan, Y. NegishiandT. Pal, *ACS applied materials & interfaces*, 5 (2013) 8724
12. L. Fu, Y. ZhengandA. Wang, *Int. J. Electrochem. Sci*, 10 (2015) 3518
13. Y. Zheng, L. Fu, A. WangandW. Cai, *Int. J. Electrochem. Sci*, 10 (2015) 3530
14. F. Han, H. Li, J. Yang, X. CaiandL. Fu, *Physica. E*, 77 (2016) 122
15. M.J. Allen, V.C. TungandR.B. Kaner, *Chemical reviews*, 110 (2009) 132
16. S. Dutta, S. Sarkar, C. RayandT. Pal, *RSC Advances*, 3 (2013) 21475
17. L. Fu, T. Xia, Y. Zheng, J. Yang, A. WangandZ. Wang, *Ceram. Int.*, 41 (2015) 5903
18. S.-S. Li, A.-J. Wang, Y.-Y. Hu, K.-M. Fang, J.-R. ChenandJ.-J. Feng, *Journal of Materials Chemistry A*, 2 (2014) 18177
19. J. JiangandX. Du, *Nanoscale*, 6 (2014) 11303
20. J.-J. Lv, S.-S. Li, A.-J. Wang, L.-P. Mei, J.-R. ChenandJ.-J. Feng, *Electrochimica Acta*, 136 (2014) 521
21. L. Fu, Y. Zheng, Q. Ren, A. WangandB. Deng, *Journal of Ovonic Research*, 11 (2015) 21
22. Y. Zhang, N. Zhang, Z.-R. TangandY.-J. Xu, *J Phys Chem C*, 118 (2014) 5299
23. W.S. HummersandR.E. Offeman, *Journal of the American Chemical Society*, 80 (1958) 1339
24. Z.-J. Fan, W. Kai, J. Yan, T. Wei, L.-J. Zhi, J. Feng, Y.-m. Ren, L.-P. SongandF. Wei, *ACS Nano*, 5 (2010) 191
25. J. Zhang, H. Yang, G. Shen, P. Cheng, J. ZhangandS. Guo, *Chemical Communications*, 46 (2010) 1112
26. S. Bose, T. Kuila, A.K. Mishra, N.H. KimandJ.H. Lee, *Journal of Materials Chemistry*, 22 (2012) 9696
27. J.I. Paredes, S. Villar-Rodil, A. Martínez-AlonsoandJ.M.D. Tascón, *Langmuir*, 24 (2008) 10560
28. D. Li, M.B. Muller, S. Gilje, R.B. KanerandG.G. Wallace, *Nat Nano*, 3 (2008) 101

29. Y. Zheng, A. Wang, H. Lin, L. FuandW. Cai, *RSC Advances*, 5 (2015) 15425
30. M. Seah, G. SmithandM. Anthony, *Surface and interface analysis*, 15 (1990) 293
31. T.D. ThomasandP. Weightman, *Physical Review B*, 33 (1986) 5406
32. A. Umar, M.M. Rahman, S.H. KimandY.-B. Hahn, *Chemical Communications*, (2008) 166
33. B. Fang, C. Zhang, W. ZhangandG. Wang, *Electrochimica Acta*, 55 (2009) 178
34. C. Wang, L. Zhang, Z. Guo, J. Xu, H. Wang, K. ZhaiandX. Zhuo, *Microchim. Acta.*, 169 (2010) 1
35. E.F. Perez, G.d.O. Neto, A.A. TanakaandL.T. Kubota, *Electroanalysis*, 10 (1998) 111